**Desalination & Water Purification Research and Development Program Report No. XXX**

# Mesophase Templated Porous Polymers as Ultrafiltration Membrane

**Prepared for Reclamation Under Agreement No. R10AC80283**

*by*

**Sahar Qavi, Reza Foudazi**

# MISSION STATEMENTS

The mission of the Department of the Interior is to protect and provide access to our Nation's natural and cultural heritage and honor our trust responsibilities to Indian tribes and our commitments to island communities.

The mission of the Bureau of Reclamation is to manage, develop, and protect water and related resources in an environmentally and

# Disclaimer

The views, analysis, recommendations, and conclusions in this report are those of the authors and do not represent official or unofficial policies or opinions of the United States Government, and the United States takes no position with regard to any findings, conclusions, or recommendations made. As such, mention of trade names or commercial products does not constitute their endorsement by the United States Government.

# Acknowledgements

The authors would like to thank the U.S. Bureau of Reclamation for providing funding through IEE/NMSU cooperative agreement, Dr. Millicent Firestone at the Center for Integrated Nanotechnologies (CINT) in Los Alamos National Laboratory for helping in Small-angle X-ray Scattering measurements, and New Mexico State University for start-up package.

## Contents

## Table of Figures

## Glossary

| Term | Description |
|---|---|
| $I_1$, $L_1$ | Normal micellar cubic phase |
| $H_1$ | Normal hexagonal mesophase |
| $L_\alpha$ | Lamellar mesophase |
| K, $V_2$ | Gyroid mesophase |
| $H_2$ | Reverse hexagonal mesophase |
| $I_2$, $L_2$ | Reverse micellar cubic phase |
| Q | Scattering vector (1/Å) |
| G' | Storage modulus (Pa) |
| G" | Loss modulus (Pa) |
| η* | Complex viscosity (Pa.s) |
| UF | Ultra filtration |
| PEO | Poly(ethylene oxide) |
| PPO | Poly(propylene oxide) |
| AIBN | Azobisisobutyronitrile |
| EGDMA | Ethylene glycol dimethacrylate |
| CTAB | Cetyletrimethylammonium bromide |
| BA | Butyl acrylate |

| | |
|---|---|
| K | Darcy's constant ($m^2$) |
| L | Membrane thickness (μm) |
| Q | Flow rate ($m^3/s$) |
| M | Feed viscosity (Pa.s) |
| A | Membrane area ($mm^2$) |
| ΔP | Pressure difference along the membrane (Pa) |
| R | Rejection |
| $C_p$ | Permeate concentration (g/L) |
| $C_f$ | Feed concentration (g/L) |

## Executive Summary

Clean water scarcity is the number one critical problem in the world. Increasing population gives rises to clean water demand and wastewater production, and thus, further development of water treatment methods. Ultrafiltration is a necessary step for treating the wastewater, in which suspending particles, viruses, and bacteria are removed. Conventional ultrafiltration (UF) membranes are produced by non-solvent induced phase separation (NIPS) technique; but, this method is not ecofriendly and the resultant membranes are anisotropic with low surface area and porosity.

Self-assembly of block copolymers in oil/water interface have been widely studies due to its wide range of potential applications in technology and science. The purpose of this research is to utilize self-assembly as a template for producing mesoporous polymeric materials that can be used as UF membranes.

In order to study the self-assembly of block copolymers in oil/water interface, different compositions of water/oil/surfactant were studied by changing the monomer and surfactant types and concentrations. Both small molecule surfactants and polymeric surfactants were used in the study. The oil used in this study comprised of butyl acrylate and ethylene glycol dimethacrylate, which can be polymerized by photo and thermal initiators. Ethylene glycol dimethacrylate in the formulations works as cross-linker to provide integrity and appropriate mechanical properties. After forming desired structures of mesophases, oil phase was polymerized to obtain a mesoporous polymer. Polarized light microscopy (PLM), rheology, and small angle X-ray scattering (SAXS) have been used for characterization of the resultant materials. The produced membranes have mesopores in the range of 70 nm and show improved permeability compared to conventional UF membranes. Permeability of membranes was measured in a dead-end flow using a home-made device.

## 1. Water scarcity

Water resources become scarcer as the world population continues to grow. Based on United Nation statistics, by 2025, 1.8 billion people will be living in countries or regions with absolute water scarcity, and two-thirds of the world's population could be living under water stressed conditions. Additionally, with the existing climate change scenario, almost half of the world's population will be living in areas of high water stress by 2030, including between 75 million to 250 million people in Africa. Water scarcity in some arid and semi-arid places will displace between 24 million and 700 million people.[1]

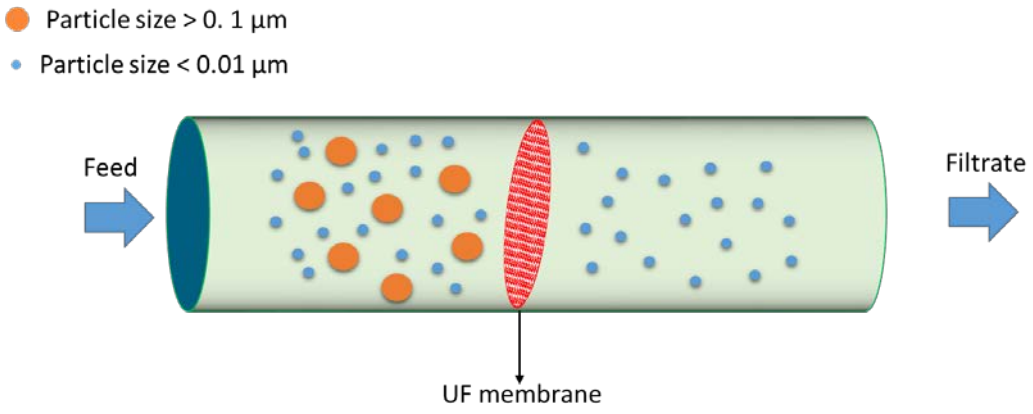


Figure 1. UF membrane can filter particles and impurities in the range of >0.1 µm.

Increase in water usage will raise the amount of wastewater that should be treated sufficiently to meet the environmental regulations. Water treatment processes employ several types of membranes, including microfiltration (MF),

ultrafiltration (UF), nanofiltration (NF), and reverse osmosis (RO).[2] These processes are usually employed in series in order to purify water efficiently. Figure 1 shows a schematic of a UF membrane. UF uses a finely porous membrane and is a pressure-driven process. Typical UF membranes have the pore size diameter of 0.01-0.1 μm and are used as a pretreatment before NF and RO processes in order to remove proteins, organic acids, oil emulsions, microbes, and viruses from wastewater.

### 1.1. Non-solvent induced phase separation method

Phase inversion techniques are among the most important and commonly used processes for preparing membranes from a large number of polymeric building blocks. Development of integrally skinned asymmetric membranes by Loeb and Sourirajan in the 1960s is a major breakthrough in membrane technology.[3] Over the past half century, a plethora of knowledge has been generated about phase inversion membranes formed by immersion precipitation, also known as non-solvent induced phase inversion (NIPS).

Many different polymers are used in the synthesis of microfiltration, ultrafiltration, nanofiltration, and reverse osmosis membranes using NIPS method. Polysulfone (PSf), polyethersulfone (PES), polyacrylonitrile (PAN), cellulosics, poly(vinylidene fluoride) or PVDF, poly(tetrafluoroethylene) or PTFE, polyimides (PI), and polyamides (PA) are among the most common polymeric membrane materials in use today.[4]

Polysulfone (PSf) is one of the most common polymers used to make membranes by phase inversion process. Polysulfone is often selected because of its commercial availability, ease of processing, favorable selectivity-permeability characteristics, and glass transition temperature ($T_g$) value of 190°C. It possesses good mechanical, thermal, and chemical properties. Moreover, it is generally easy to prepare asymmetric membranes by the phase inversion method, in which a thin layer of PSf solution in an appropriate solvent is immersed into the non-solvent coagulation bath, such as water. The most frequently used solvents for PSf are N-methylpyrrolidone (NMP),[5] N,N-dimethylacetamide (DMAc),[6] and N,N-dimethylformamide (DMF).[7]

In NIPS method, the base polymer for membrane production should be dissolved in a significant amount (more than 65 wt.%)[7] of an organic solvent, which makes the process indeed non-ecofriendly. Moreover, the polymer solution should be usually dilute, and therefore, the process is not efficient in time, energy and raw material consumption. The thickness of membranes produced by NIPS method is limited since a polymer solution film should coagulate through immersion in a non-solvent to form membrane. A development objective that can hardly be achieved by NIPS is to produce 2-3 mm diameter capillary fiber modules which is necessary to lead to lower energy consumption and higher, more stable membrane fluxes.[2] Therefore, there is a growing need for producing new levels of hierarchical membranes and alternative methods for membrane production with emphasis on ecofriendly processes, higher flux and/or lower operational pressure, and less expensive processes for wastewater treatment and filtration

processes for industrial applications. One alternative method is tempelating approach for producing mesoporous materials that will be covered in next section.

### 1.2. Templating approach for synthesis of porous materials

According to the definition of the International Union of Pure and Applied Chemistry (IUPAC), porous materials can be classified into microporous (with pore diameter <2 nm), mesoporous (2–50 nm) and macroporous (>50 nm) materials, respectively.[8] In the case of mesoporous materials, the structural capabilities at the scale of a few nanometers and high surface area can meet the demands of the growing applications such as adsorption, separation, catalysis, drug delivery, sensors, photonics, energy storage and conversion, and nanodevices. Direct templating by preformed lyotropic liquid crystal (LLC) phases prepared under relatively high surfactant concentrations has been widely used for producing mesoporous oxides, such as silica and niobium oxide.[9,10]

Inorganic mesoporous materials are limited in terms of processability and mechanical strength.[11] Such limitations can be overcome through organic mesoporous materials, which have chemical tunability, mechanical properties, and processability coupled with the high surface area, stability, and reactivity.[12,13]

When polymerizable surfactants[14] are used templating process is called **'synergistic'** and the material obtained is the cured template. On the other hand,

a **'transcriptive'** synthesis results in a product that is a copy of the template structure, for example when monomer polymerizes around the self-assembled surfactants. In some cases even when the template structure is not retained during polymerization the self-organized reaction medium can still direct polymer growth. In this way, new and typically hierarchically morphologies are formed. Such cases of indirect templating are called **'reconstructive'** synthesis.[15,16]

Templating within organized solutions is a much more complex process than that Hentze et al.[16] suggested by the simple picture of 'casting' a surfactant assembly. Polymerization reaction progresses within a highly dynamic self-organized medium in a continuously changing physico-chemical environment. As the monomer phase is substituted by a polymer phase, changes of the polarity of the dispersion medium and the partitioning of each compound may occur. Many monomers show some degree of surface activity and consequently segregate at the assembly's interface.[16]

Polymerization can cause phase transitions by driving changes in the interface curvature. More severe effects arise due to the loss of entropy or chemical incompatibility of the polymer with the surfactant, and this sometimes drives phase separation and concomitant disruption of the initial structure. In these cases, the surfactant phase still coexists with the demixed polymer phase, so there are usually no significant changes of optical textures or diffractograms recorded before and after polymerization.[16]

Given the dilemma that polymerization-induced phase separation is always the enemy of direct synergistic or transcriptive templating, two strategies can be developed for the synthesis of ordered supramolecular materials. One is to suppress phase separation by adjusting thermodynamic and kinetic parameters, either in the original formulation or, perhaps, by changing conditions as the reaction proceeds. To do so, several approaches have been proposed by Hentze and Kaler as follows:[16]

(i) kinetic stabilization by the use of surfactants with slower exchange dynamics (e.g. amphiphilic block copolymers);

(ii) polymerization within templates with long rearrangement times (e.g. hexagonal and cubic phases);

(iii) thermodynamic adjustment of the surfactant/monomer/polymer mixture (e.g. by matching the molecular structure to induce some attractive interaction, and thus, compatibility); and

(iv) cross-linking of the polymer matrix to 'compensate' for the entropy loss caused by producing the polymer matrix in a confined nanogeometry (e.g. monomers with a high number of reactive entities per molecule cross-links upon polymerization, and small multifunctional monomers such as divinylbenzene can be added to mono-functional monomers to form cross-linked networks).

Another strategy for the synthesis of ordered materials, not yet fully developed, is to make use of the high sensitivity of the interaction between polymer network chemistry and surfactant mesophase chemistry. When aiming at the

reconstructive templating of polymers with even more complex morphologies, this sensitivity can be used as a powerful tool for the synthesis of new hierarchical polymer structures. One example is the colloidal ordering of polymer gels by polymerization-induced phase separation within inverse hexagonal phases.[17]

Gin and Gu[12] have used cross-linked lyotropic liquid crystal (LLC) phases as catalysts in the development of systems capable of acid catalysis. LLC phases are self-assemblies of amphiphilic molecules that form in a solvent. However, unlike micelles and vesicles which are relatively simple individual structures, LLC phases are highly ordered yet fluid condensed assemblies with specific nanometer-scale geometries. The tails of the amphiphiles in LLC phases form fused hydrophobic regions while the hydrophilic (typically ionic) headgroups define the interfaces of ordered, extended aqueous regions. Depending on the shape of the LLCs and the interfacial curvature, aqueous domains ranging from lamellae to cylindrical channels with dimensions in the 1-10 nm range can be formed.[18]

Considerable difficulties arise in templating LLC structures onto organic polymers. It is entropically unfavorable for polymers to exist in the confined dimensions of LLC phases, and thus, phase separation can occur. The sizes of morphologies generated are often in nanometer range, but not the same as the original LLC structure due to uncontrolled phase separation.[16,19]

Some researches on the polymerization in LLC media have yielded mixed results as lyotropic structures are not typically retained or are significantly altered upon polymerization.[20–22] On the other hand, a limited number of cases have been

reported showing retained LLC structure upon polymerization. For example, O'Brien et al. polymerized a dienoyl phospholipid in the inverted hexagonal phase with retention of the original lyotropic structure.[23]

Lester et el.[13] have studied the kinetic of photopolymerization in LLC media. They have shown that reactions in the ordered structure of LLC are highly dependent on the type and degree of order, and are significantly different than in an isotropic state. This phenomenon can be attributed to a number of factors including diffusional limitation which reduce termination rates and segregation of the monomeric species increasing both the apparent propagation and termination values.[24]

## 1.3. Self-assembly of amphiphilic block copolymers in oil/water interface

Surface-active agents (surfactants) can self-assemble in water/oil mixtures to form mesomorphic phases (mesophases), which are anisotropic structures highly extended in one or two dimensions.[25,26] Surfactant molecules play a vital role in the formation of mesophases and their stability. Small molecule surfactants have been widely used in several applications for producing mesophase structures.

A polymer is a large molecule, or macromolecule, composed of many repeating units (mer). Copolymers are synthesized by polymerization of more than one type of monomer. If copolymer molecule consists of blocks of different monomers, the resultant copolymer is called a block copolymer. The blocks in

copolymer can be incompatible with one another, e.g. in amphiphilic block copolymers. Literally, amphiphilic means loving both and amphiphilicity can be expressed toward any two solvents which are incompatible with each other, oil and water for instance. Amphiphilic block copolymers have a wide range of applications in pharmaceutical, cosmetics, drug delivery, and catalysis.[27] Amphiphilic block copolymers can be used as surfactants at oil/water interfaces as well. Similar to conventional low molar mass surfactants, amphiphilic block copolymers may form micelles, vesicles, or lyotropic mesophases. While polymeric surfactants are less studied than small-molecule surfactants for self-assembly, they offer some opportunities in terms of flexibility, diversity, and functionality.[28] Additionally, polymeric amphiphiles self-assemble to structures which are more stable, and have a lower critical micelle concentrations (CMC) compared to their small molecule analogues.[29] After all, the block composition is the main determinant of the microstructure observed in solvent-free block copolymers[30,31] as the chemical composition of typical surfactants ("head group" and "tail") affects their hydrophilic/lipophilic ratio and self-assembly in solution properties.

Pluronic block copolymers are triblock copolymers of poly (ethylene oxide) (PEO) and poly (propylene oxide) (PPO), often denoted as PEO-PPO-PEO or $(PEO)_X$-$(PPO)_Y$-$(PEO)_Z$, are nonionic polymeric surface active agents. Figure 2 shows the chemical structure of typical Pluronic block copolymers. Variation of copolymer composition (PPO/PEO ratio) and molecular weight (PEO and PPO block length) during synthesis leads to the production of molecules with optimum properties

that meet the specific requirements in various areas of technological significance.[32]

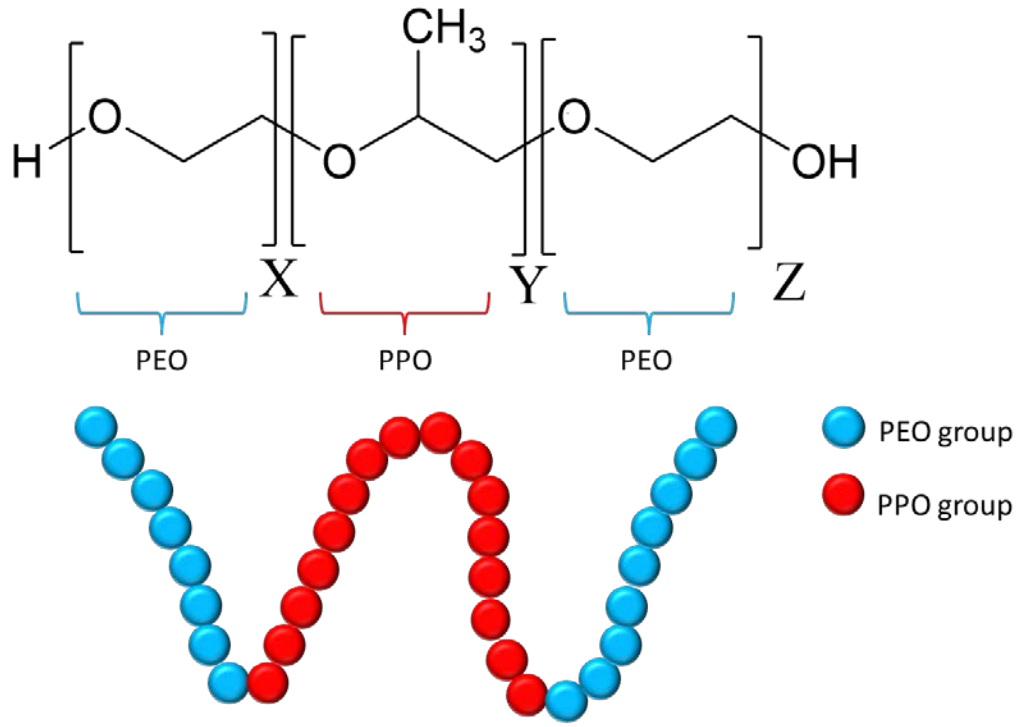


Figure 2. Chemical structure and schematic representation of a Pluronic block copolymer. X, Y, and Z show the degree of polymerization of different blocks.

The Pluronic block copolymers are available in a range of molecular weights and PPO/PEO composition ratios, with relatively low price (compared to small molecule surfactants), low toxicity and stability over a wide pH range.[33,34] The notation for the Pluronic triblock copolymers starts with the letters L (for liquid), P (for paste), or F (for flakes) followed with a number. The first one or two numbers are indicative of the molecular weight of the PPO block, and the last

number signifies the weight fraction of the PEO block.[32] For example, Pluronic F127 and Pluronic L121, have the same molecular weight of PPO, but F127 has 70 wt.% PEO and L121 has 10 wt.% PEO.

Solvent-free block copolymers can self-assemble as spheres, cylinders, and lamellae, similar to small molecule surfactants in solution.[35] In the presence of water or in ternary systems with water and oil, PEO/PPO copolymers can self-assemble into lyotropic liquid crystalline structures.[36,37] Alexandridis et al.[32,38,39] initiated comprehensive studies on the phase behavior and microstructure of ternary systems consisting of an amphiphilic Pluronic block copolymer and two solvents, one (water) selective for the PEO blocks and another (hydrophobic oil such as p-xylene) selective for PPO block. A rich structural polymorphism has been observed in such ternary copolymer/water/oil systems, with the block copolymer molecules self-assembling to form micro-domains with spherical, cylindrical, or lamellar geometry, discrete or interconnected topology, and liquid-crystalline organization.[40–42]

Alexandridis et al.[40] have examined the ternary phase behavior of Pluronic L64, $(PEO)_{13}$-$(PPO)_{30}$-$(PEO)_{13}$, in the presence of water and p-xylene as selective solvents of PEO and PPO, respectively. Figure 3 shows the phase diagram of such system. In addition, the ternary phase diagram of water/oil/CTAB is shown for comparison as well. CTAB stands for commonly used small molecule surfactant, cetyl trimethylammonium bromide. Progression of structure in block-copolymer/water/oil phase diagram can be discussed at two levels: i) varying water/oil ratio at constant total copolymer content, and ii) changing total

copolymer content at constant copolymer/oil [copolymer/water] ratio. It can be seen that using different compositions of water/p-xylene in constant surfactant fraction or using different surfactant/water (or surfactant /oil) ratios in constant oil (or water) composition leads to various liquid crystalline structures. $L_1$, $H_1$, $L_\alpha$, $V_2$, $H_2$, and $L_2$ denote normal (oil-in-water) micellar solution, normal hexagonal, Lamellar, reverse bicontinuous cubic, reverse (water-in-oil) hexagonal, and reverse micellar solution, respectively (all listed in Glossary).

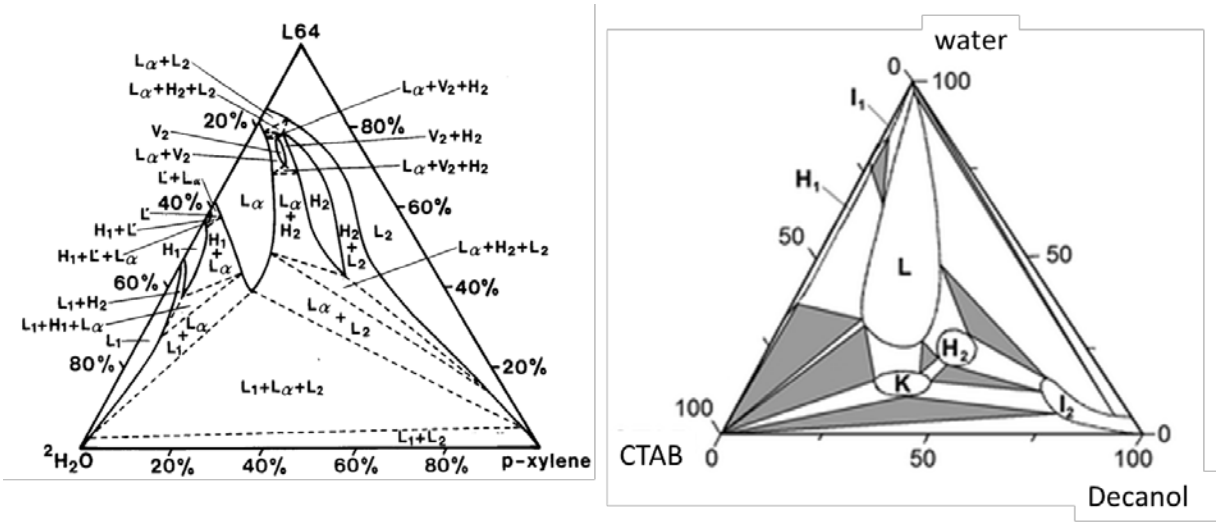


Figure 3. Phase diagram of the water/p-xylene/ Pluronic L64 block copolymer[40] and water/decanol/CTAB[43]

The type of structure obtained does not only depend on the ternary copolymer-water-oil composition, but also depends on the PEO/PPO ratio and molecular weight of block copolymer. The ability of the blocks to swell to different extents (based on the amount of solvent available) modulates the interfacial "curvature", and thus, the resulting structure. An increase in the copolymer

molecular weight for a given block composition increases the block segregation (for the same solvent conditions) and results in an increase of the temperature and composition stability range of the different structures. Higher polymer molecular weight may also lead to the formation of additional structures because of the increase in the range of inter-assembly interactions.[41]

## 2. Experimental

### 2.1. Approach

In this work, we mainly study the self-assembly of Pluronic L64 block copolymer in oil/water interface and utilize its mesophases as a template for producing UF membranes. To produce mesoporous membranes, polymerizable species (monomer) are used in the oil phase of the system. After self-assembly of oil/water/Pluronic block copolymer in a desired phase state, the monomer is polymerized to obtain the designed porous structure as schematically shown in Figure 4.

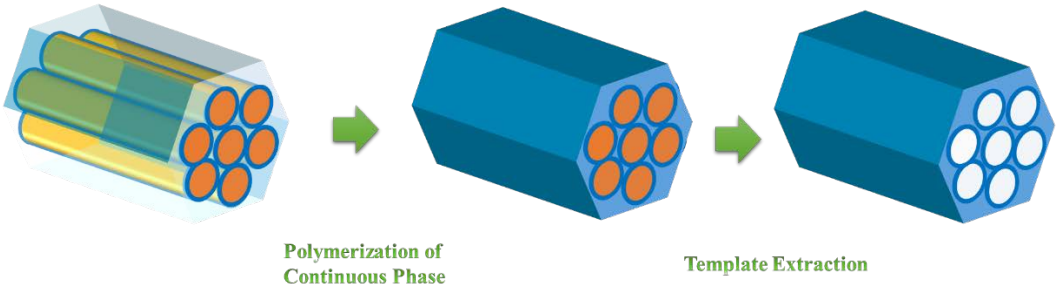


Figure 4. Templating approach for making porous materials

## 2.2. Materials

Poly(ethylene oxide)-b-poly(propylene oxide)-b-poly(ethylene oxide), Pluronic L64, was kindly provided by BASF corporation. Butyl acrylate (≥99%), 4,N,N-trimethylaniline (≥98.5%), azobisisobutyronitrile (98%), 1-hydroxycyclohexyl phenyl ketone (99%), and cetyletrimethylammonium bromide (CTAB, ≥98%) were obtained from Sigma-Aldrich. Ethylene glycol dimethacrylate was purchased from Electron Microscopy Sciences. Benzoyl peroxide was obtained from Fisher Scientific. All chemicals were used as received.

Butyl acrylate (BA) and ethylene glycol dimethacrylate (EGDMA) were used as monomer and cross-linker, respectively. 1-Hydroxycyclohexyl phenyl ketone and azobisisobutyronitrile (AIBN) were used as UV and thermal initiators, respectively. 4,N,N-trimethylaniline and benzoyl peroxide were used as redox initiation system. Chemical structures of small molecule surfactant, block copolymer, monomer, cross-linker, and initiators are shown in Figure 5. The amounts of cross-linker and initiators in the oil phase were kept constant for different compositions.

The experiment comprises of two steps: (i) a simple mixing of all materials in which no chemical reaction takes place, and (ii) a cross-linking polymerization process in which a porous polymeric network (membrane) are formed. For the first step, desired amount of monomer, cross-linker, and initiator were mixed together and centrifuged at alternative directions for several times until a transparent gel (the mesopahse) was obtained. Then, mesophases were placed in a UV chamber (Spectrolinker™ XL-1000) in the optimum intensity mode for 4

hours. After that, pre-cured samples were placed in drying oven at 60 °C for 3 hours until they were cured completely.

Talc powder and oil-in-water emulsion were used to evaluate the rejection performance of the membranes. 2 g talc powder was dissolved in 1 L water and the suspension was stirred for 30 minutes. 0.5 g NaCl and 5 g Pluronic F 68 were added to stabilize the suspension. Talc suspension was used as feed stream. Talc concentration in the feed and permeate was measured and solute particle rejection was calculated. In order to calculate the permeate concentration, permeate was centrifuged at the speed of 11000 rpm for 15 minutes using an Eppendorf centrifuge model 5804 (Figure 6).

Rejection performance was also tested using an oil-in-water emulsion as feed. Vegetable oil and Pluronic F68 were used as oil phase and surfactant, respectively. First, 1 g Pluronic F68 was added to 1 L DI water and stirred for 15 minutes until it was completely dissolved in water. Then, 25 g vegetable oil was added drop wise (using a syringe pump) to the continuously being stirred solution. Resultant oil-in-water emulsion was used to test the rejection performance of the membranes.

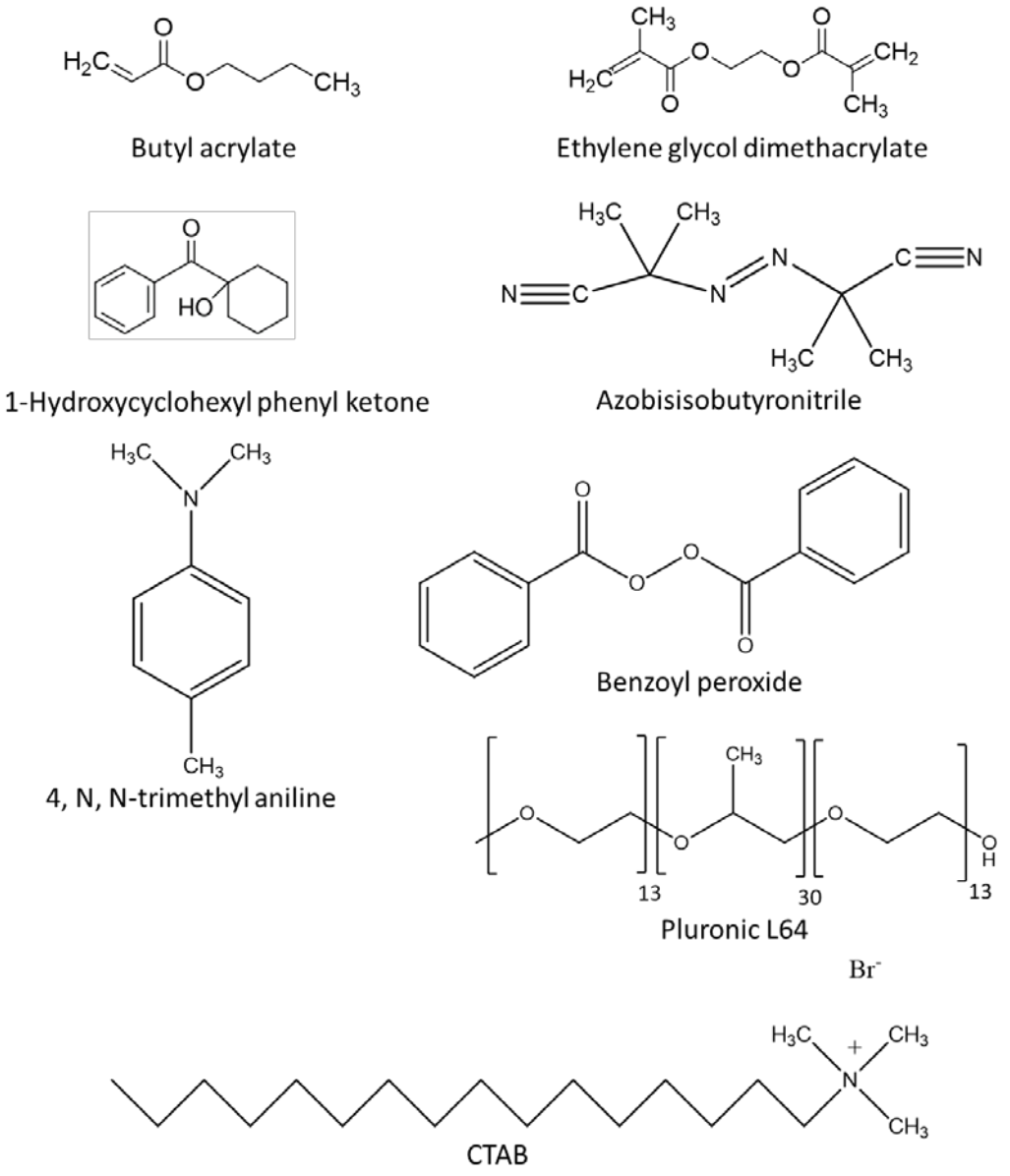


Figure 5. Chemical structures of monomer (butyl acrylate), cross-linker (ethylene glycol dimethacrylate), initiators (1-hydroxyxyclohexyl phenyl ketone, azobisisobutyronitrile, benzoyl peroxide, and 4,N,N-trimethylaniline), block copolymer (Pluronic L64), and small molecule surfactant (CTAB)


Figure 6. Eppendorf centrifuge model 5804 used for removing talc from permeate

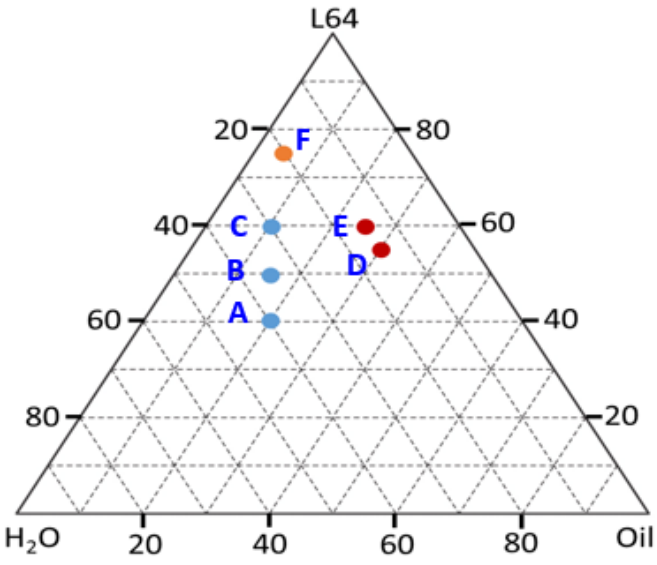


Figure 7. Six different compositions used for making mesophases from Pluronic L64.

Six compositions were chosen in the phase diagram of water/oil/Pluronic L64 to make mesophases (Figure 7). Compositions A, B, and C are expected to be in the lamellar region according to the phase diagram of water/xylene/Pluronic L64 obtained by Alexandridis.[40] Similarly, compositions D and E are expected to be in the hexagonal region and sample F is expected to be in the continuous cubic (gyroid) region.

## 2.3. Set up for making membrane

Mesophases show yield stress and do not flow under their weight as will be shown in rheological results. Therefore, processing a mesophase into a membrane needs to be done using a hot press. Such process can be scaled up to industrial scale if needed. For preparation of membranes, a small amount of the monomer gel mixture was first placed on a piece of support layer. In order to avoid biased results and conclusion originated by differences in support layers, we recovered the support from a commercial UF membrane (GE, MW series, MW2540F30) in this work, and fabricated our membranes on it. Then, the gel mixture on the support was sandwiched between Mylar sheets and placed between smooth stainless steel plates. The entire assembly was then pressed using a hot press machine pre-heated to 50 °C, by applying a force of 15 tons for five minutes to infuse the monomer mixture completely through the support layer. For photopolymerization, the resulting infused film (still between Mylar sheets) was placed in the UV chamber for four hours. Afterwards, the film was placed in a drying oven at 70 °C to complete the polymerization (Figure 8).

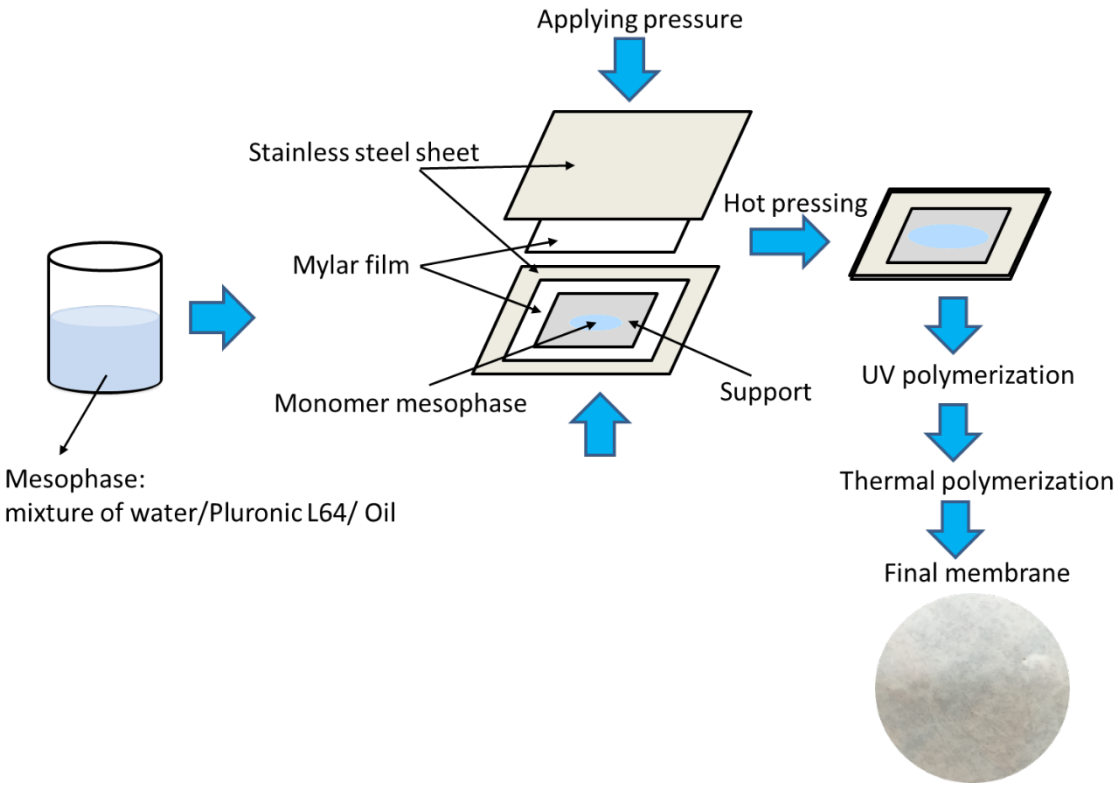


Figure 8. Processing mesophase to make membrane

## 2.4. Characterization techniques

### 2.4.1. Polarized light microscopy (PLM)

Olympus microscope (model BX60) with cross-polarized feature was used to characterize the liquid crystalline structure of mesophases before and after the polymerization. A small amount (less than 2 ml) of each mesophase sample (before polymerization) was placed on a glass slide and was covered with cover slip. The cross-polarized images of samples were recorded using a camera

attached to the microscope. In order to characterize samples after polymerization, each mesophase was polymerized on the glass slide using UV initiation system for 3 hours. Obtained samples were covered by a cover slip and studied by cross-polarized light microscopy.

Cross-polarized light microscopy is basically utilized to distinguish between singly refracting (optically isotropic) and doubly refracting (optically anisotropic) media. Anisotropic substances, such as uniaxial or biaxial crystals, oriented polymers, or liquid crystals, generate interference effects in the polarized light microscope, which result in differences of color and intensity in the image as seen through the eyepieces and captured on digital image. This technique is useful for orientation studies of doubly refracting media that are aligned in a crystalline lattice or oriented through long-chain molecular interactions in natural and synthetic polymers.[44]

Lamellar mesophases exhibit distinct optical texture, when confined in thin slabs between crossed polarizers. Typically, the texture is 'streaky' or mosaic-like (to quote the late Krister Fontell[45]), which resembles the marbling in freshly cut steak. Bicontinuous cubic liquid crystals exhibit symmetry and do not display optical texture. Hexagonal mesophases are often identified by a characteristic 'fan' texture in the optical microscope, due to focal conic domains of columns.[45]

### 2.4.2. Small angel X-ray scattering

Since the pore size of mesoporous materials are in the nanometer range, their structure cannot be seen through current electron microscopes available at New

Mexico State University. In addition, microscopic images are very local and may not reveal the overall structure of prepared mesophase and mesoporous material. Therefore, small angel X-ray scattering (SAXS) measurements, as also frequently used in literature,[40] were performed in this work. SAXS is an analytical method to determine the structure of mesophase systems in terms of averaged size or shape. In this method, X-rays are sent through the samples and will be scattered as they hit particles that happen to be inside the beam. Thus, the average structure of all illuminated particles in the bulk material is measured. Different structures with long-range order have different SAXS patterns, and thus, can be characterized by this technique.

Figure 9 shows a typical SAXS pattern. q is the scattering vector and its dimension is reciprocal length. Q can be calculated based on the following formula:

$$q = \frac{4\pi}{\lambda}\sin(\theta)$$

where λ and θ are X-ray wavelength and scattering angle, respectively. Distance between the aligned structures can be calculated based on Bragg's law as follows:

$$d_{Bragg} = \frac{2\pi}{q_{peak}}$$

where $d_{Bragg}$ and $q_{peak}$ are distance between the structures and scattering vector at a specific peak, respectively.

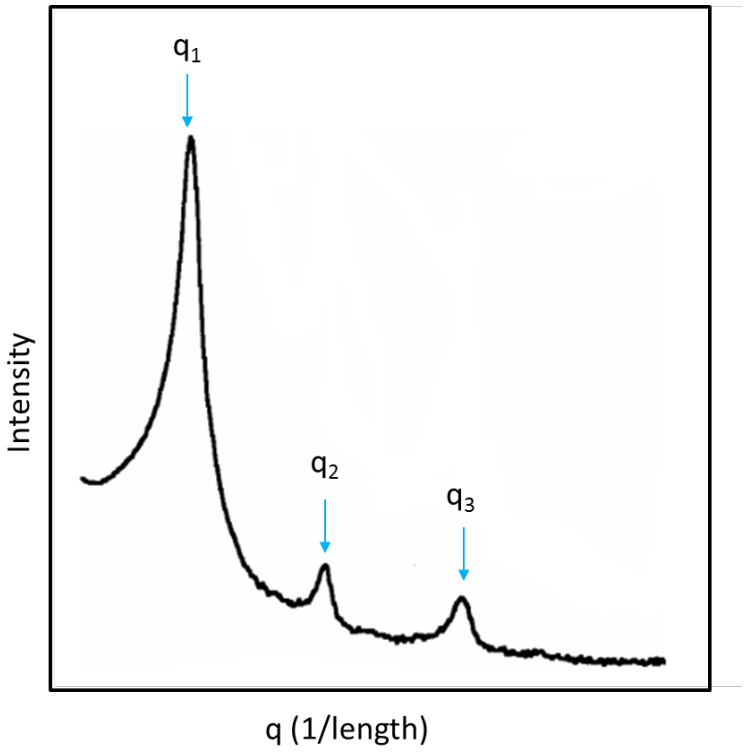


Figure 9. A typical SAXS pattern. $q_1$ is the principal peak and $q_2/q_1$ and $q_3/q_1$ ratios determine the type of crystal symmetry

The structure factor of a crystalline substance is normally called lattice factor. It is a set of peaks at well-defined angles indicative for the crystal symmetry. It can be shown that the ratios of the peak positions on the q-scale have typical values, which reveal the crystal symmetry, for example:

- Lamellar symmetry: 1, 2, 3, 4, 5, …
- Cubic symmetry: 1, $\sqrt{2}$ , $\sqrt{3}$, 2, $\sqrt{5}$, …
- Hexagonal symmetry: 1, $\sqrt{3}$, 2, $\sqrt{7}$, 3, …

The samples used for SAXS measurements were filled into a quartz capillary using centrifugation. The cuvette is stoppered using critoseal and epoxy glue. Mesophases were cured in the capillary tubes. SAXS spectra were obtained with a Bruker Nanostar system (located at Los Alamos National Lab) using a monochromated $CuK_{\alpha}$ radiation source with wavelength of 1.54184 Å. The $2\theta$ angle range of 0.1 to 4.7 was used for measurements.

### 2.4.3. Rheology

Rheological measurements were done using a discovery hybrid rheometer (DHR-3, TA Instruments). Figure 10 shows the device we used for rheometry. Mesophases are viscoelastic materials and rheometry can be used to measure their viscosity, shear modulus (G'), and loss modulus (G"). In this work, we show that each mesostructure has a rheological fingerprint, so they can be characterized by rheometry. All rheometry measurements were performed at 25 °C. A parallel plate geometry with 40 mm diameter and 1 mm gap was used for all tests. Amplitude sweep measurements were done using an angular frequency of 10 rad/s and over strain range of 0.01 to 1000%. Frequency sweep were performed using a strain amplitude of 1% and over a frequency range of $\omega$= 0.01 to 600 rad/s. Non-linear rheological measurements were performed using amplitude oscillation with sampling time of 10 cycles and conditioning time of 5 cycles.

Figure 10. DHR-3 device used for rheometry

### 2.4.4. Permeability

Permeability of membranes was measured using a home-made device (Figure 11). The membrane discs were assembled into a stainless steel dead-end filtration cell with an inner diameter of 25 mm and an effective filtration area of 1380 $mm^2$.

Darcy's law was used to calculate the permeability as follows:

$$\frac{\kappa}{l} = \frac{Q\,\mu}{A\,\Delta P}$$

where, $Q$, $\mu$, $A$, $\Delta P$, $l$, and $\kappa$ are flow rate, viscosity, membrane area, pressure difference along the membrane, membrane thickness, and Darcy's constant (which features intrinsic permeability), respectively. The ratio of $\kappa/l$ was considered as an indication of operational permeability in this work. In other words, since different membranes have different thicknesses which is also difficult to be accurately measured, the value of intrinsic permeability itself can be misleading in real application.

Figure 11. Home-made filtration set-up

## 3. Results and discussion

Different formulations were used for making membranes. In the first set of experiments CTAB, which is a small molecule surfactant, was used. CTAB is highly sensitive to temperature and crystallizes below 30 °C. Samples containing CTAB were polymerized with strict control on the temperature. Samples before polymerization showed liquid crystalline behavior. However, small crystals started to grow inside them upon cooling down to room temperature, which results in the segregation of CTAB molecules through crystallization. Table 1 shows some of the formulations that were prepared using CTAB as surfactant.

Despite the fact that CTAB surfactant can make ordered structures in mesophases, the formulations containing CTAB were excluded from membrane fabrication due to their susceptibility to crystallization at room temperature. Pluronic L64 was used mainly in membrane fabrication as surfactant since it forms stable mesophases as it will be shown later.

First, redox initiation system was used for polymerization. Benzoyl peroxide and 4,N,N-trimethyl aniline are a hydrophobic redox pair and were used to polymerize butyl acrylate. Using this system, polymerization takes place at room temperature after about 10 minutes. For making samples, half of the ingredients were mixed with benzoyl peroxide and 4,N,N-trimethyl aniline was added to the other half. These two halves were mixed together just before applying the mesophase on the support for making membranes. The main drawback of redox system is that we could not control the rate of polymerization efficiently and membrane fabrication was not successful.

Table 1. A summary of formulations that were prepared using CTAB

| Oil/water/CTAB composition | Oil phase formulation |
|---|---|
| 30 wt%/40 wt%/30 wt% | UV initiator 7.5 wt.% of monomer<br>Cross-linker 33 wt.% of monomer |
| 10 wt%/70 wt%/20 wt% | Redox initiator 7.5 wt.% of monomer<br>Cross-linker 33 wt.% of monomer |
| 10 wt%/60 wt%/30 wt% | Redox initiator 7.5 wt.% of monomer<br>Cross-linker 33 wt.% of monomer |
| 10 wt%/50 wt%/40 wt% | Redox initiator 7.5 wt.% of monomer<br>Cross-linker 33 wt.% of monomer |
| 10 wt%/40 wt%/50 wt% | Redox initiator 7.5 wt.% of monomer<br>Cross-linker 33 wt.% of monomer |
| 20 wt%/60 wt%/20 wt% | Redox initiator 7.5 wt.% of monomer<br>Cross-linker 33 wt.% of monomer |
| 20 wt%/50 wt%/30 wt% | Redox initiator 7.5 wt.% of monomer<br>Cross-linker 33 wt.% of monomer |
| 20 wt%/40 wt%/40 wt% | Redox initiator 7.5 wt.% of monomer<br>Cross-linker 33 wt.% of monomer |
| 20 wt%/30 wt%/50 wt% | Redox initiator 7.5 wt.% of monomer<br>Cross-linker 33 wt.% of monomer |

UV initiator was used instead of redox system in the next set of experiments. The ratios of cross-linker and initiator were kept constant at 33 wt.% of monomer and 5 wt.% of monomer, respectively. UV rays diffusion inside the media is limited, and therefore, UV initiator by itself could not completely polymerize the membranes. Additionally, final membranes did not have enough integrity due to low degree of cross-linking. Therefore, in final series of experiments, the ratio of cross-linker to monomer was increased.

Table 2. A summary of oil phase formulations used to prepare water/oil/Pluronic L64 mesophases

| **Oil phase formulation** | **Comment** |
|---|---|
| Redox initiator 5 wt% of monomer<br>Cross-linker 33 wt% of monomer | Controlling the rate of polymerization is challenging. Samples were polymerized before processing into membrane. |
| UV initiator 5 wt% of monomer<br>Cross-linker 33 wt% of monomer | UV diffusion length is not enough to completely polymerize the samples. Final membrane does not have enough integrity due to low cross-linking. |
| UV initiator 5 wt% of monomer<br>Thermal initiator 5 wt% of monomer<br>Cross-linker 70 wt% of monomer | Final membranes look homogenous with enough integrity. This is the optimum formulation. |

Thermal and UV initiation systems were used in the last set of experiments in conjunction with each other to ensure that mesophases would completely polymerize. The ratios of cross-linker and initiators were kept constant at 70 wt.% of monomer and 5 wt.% of monomer, respectively. Membranes produced by such formulation have good integrity and were used as optimum samples for testing permeability and rejection. Table 2 shows a summary of different oil phase formulations that were used in this project. It should be noted that the produced formulations of mesophases had different fractions of oil phase, water, and Pluronic L64.

### 3.1. Polarized light microscopy

Figure 12 and Figure 13 show the cross-polarized micrographs obtained for mesophase prepared from CTAB and Pluronic L64 before curing, respectively. All points in Figure 11 show hexagonal textures. However, the sample with 40% CTAB goes rapidly through crystallization of CTAB, and has a different cross-polarized micrograph. As seen in the cross-polarized micrographs of Pluronic L64 mesophases shown in Figure 13, A, B, and C compositions show an oily streak texture that is the characteristic of lamellar mesophases.[45] Points D and E show focal fan texture that is the characteristic of hexagonally packed mesophases.[45] Composition F does not have any textures under PLM that could be a characteristic of gyroid type mesophase. [45]

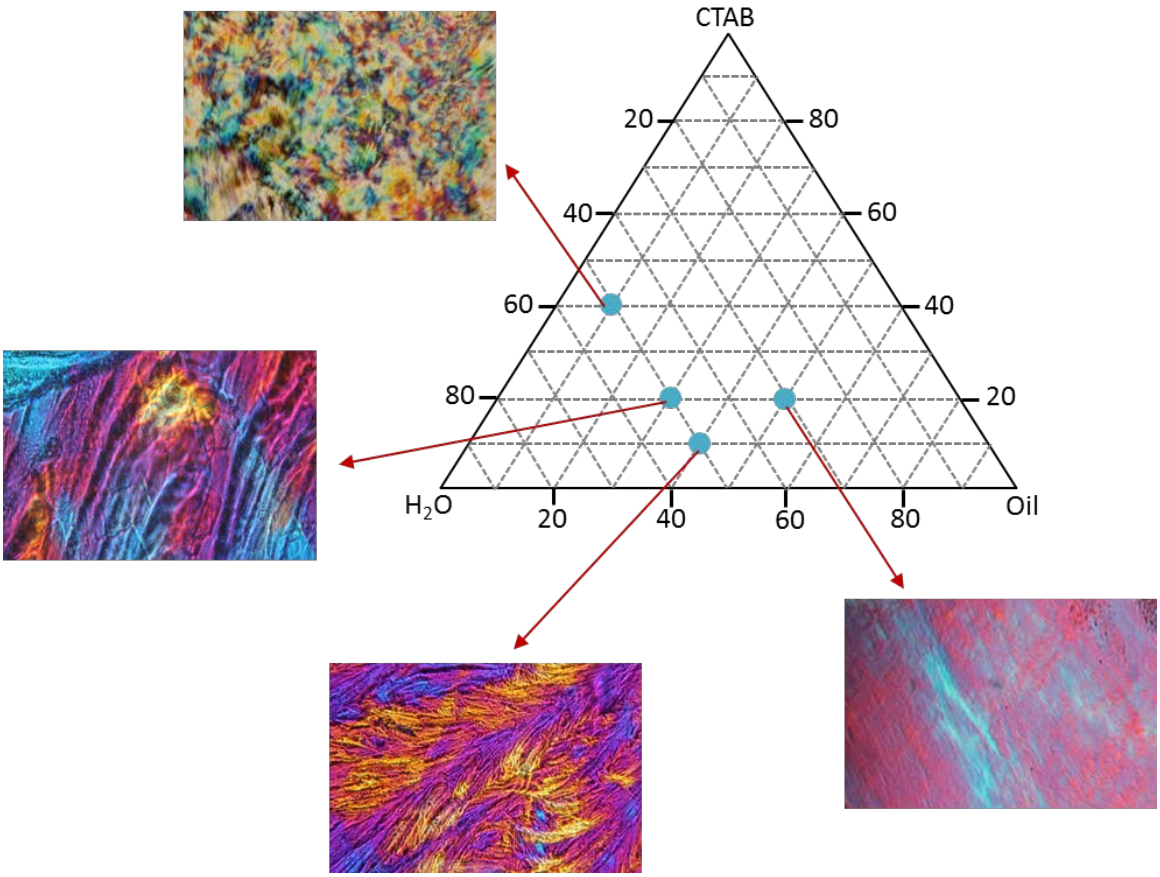


Figure 12. Cross-polarized light micrographs obtained for mesophases with different compositions containing CTAB before curing

Cross-polarized light micrographs of selected mesophases as in Figure 13 after curing are shown in Figure 14. The results show that all mesophases (except gyroid, since it may lose its structure to another non-liquid crystalline mesophase) can preserve their structure under curing. These results are promising for making membranes from mesophases since the structure does not

change during polymerization and we can expect to have a mesoporous material at the end.

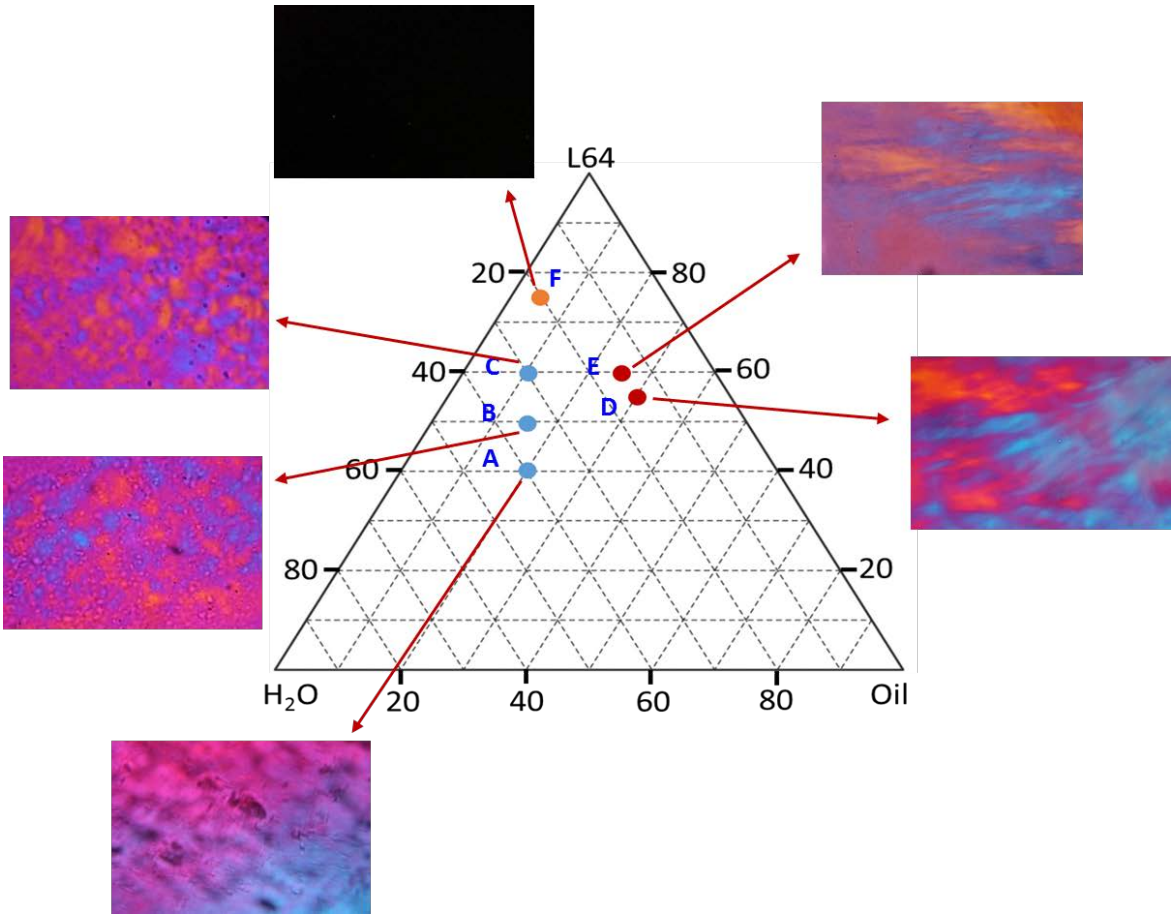


Figure 13. Cross-polarized light micrographs obtained for mesophases with different compositions containing Pluronic L64 before curing

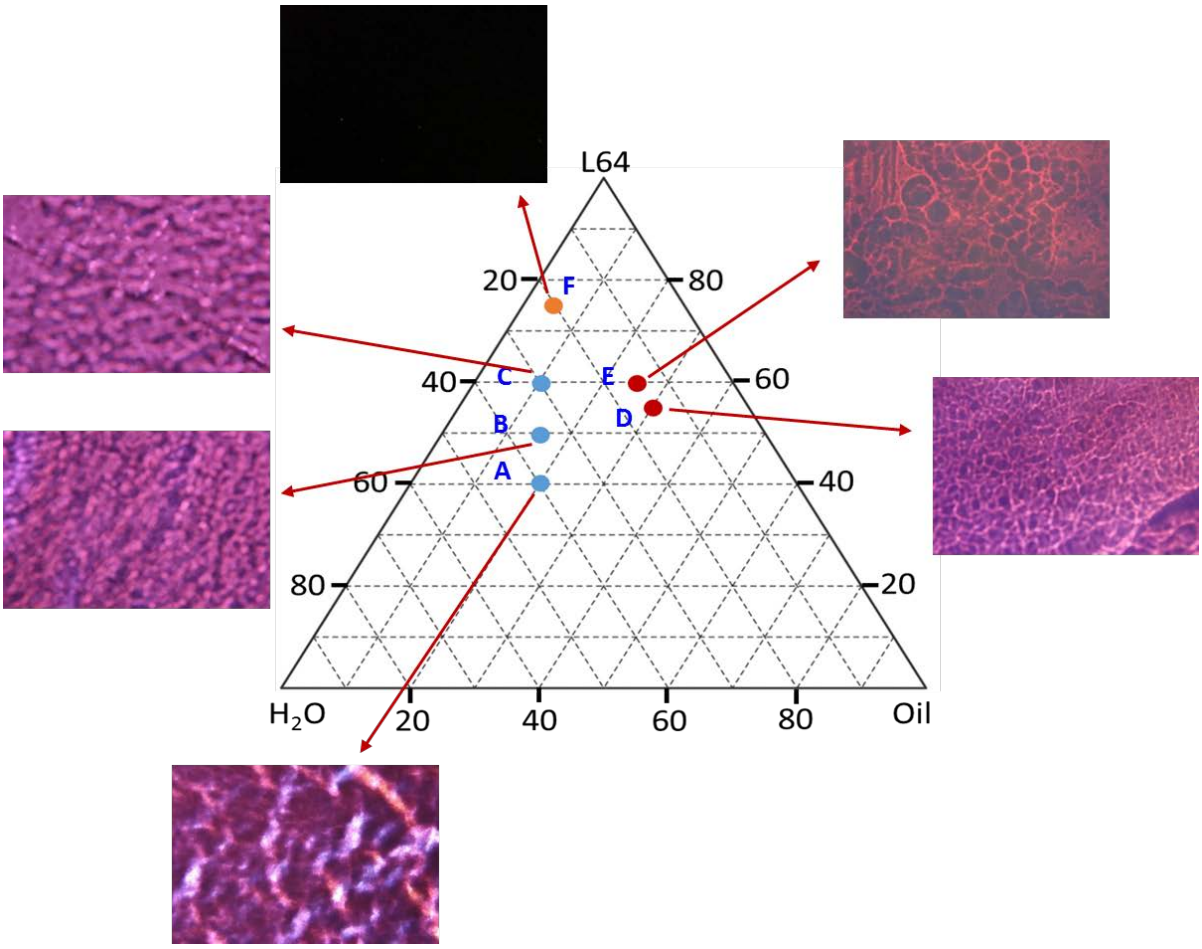


Figure 14. Cross-polarized light micrographs obtained for mesophase with different compositions containing Pluronic L64 after polymerization

## 3.2. SAXS results

SAXS studies can confirm the data obtained from PLM method. Figure 15 shows the SAXS data obtained for A, B, and C compositions. All patterns resemble the lamellar structure of mesophases. Inset images show the 2D SAXS spectrum with concentric rings which is the characteristics of lamellar mesophases.

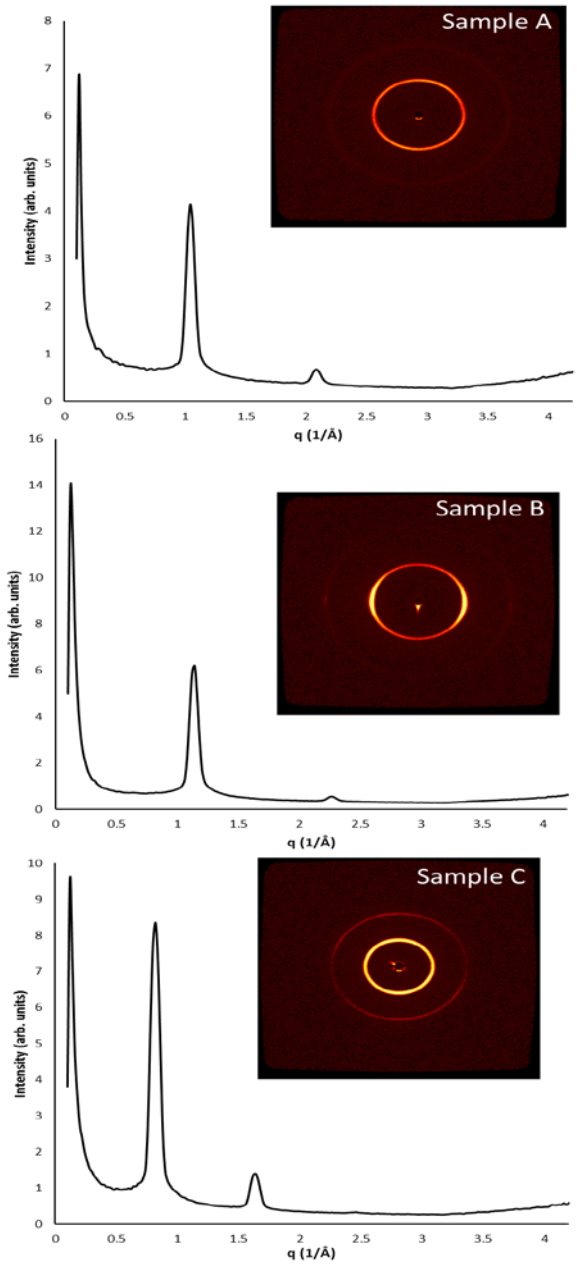


Figure 15. SAXS spectrum obtained from samples A, B, and C with lamellar pattern. Insets show 2D SAXS images

Figure 16 shows the SAXS data obtained for D and E compositions. Both patterns resemble the hexagonal structure of mesophases. Inset images show the 2D SAXS spectrum with one ring, which is the characteristic of hexagonally packed mesophases.

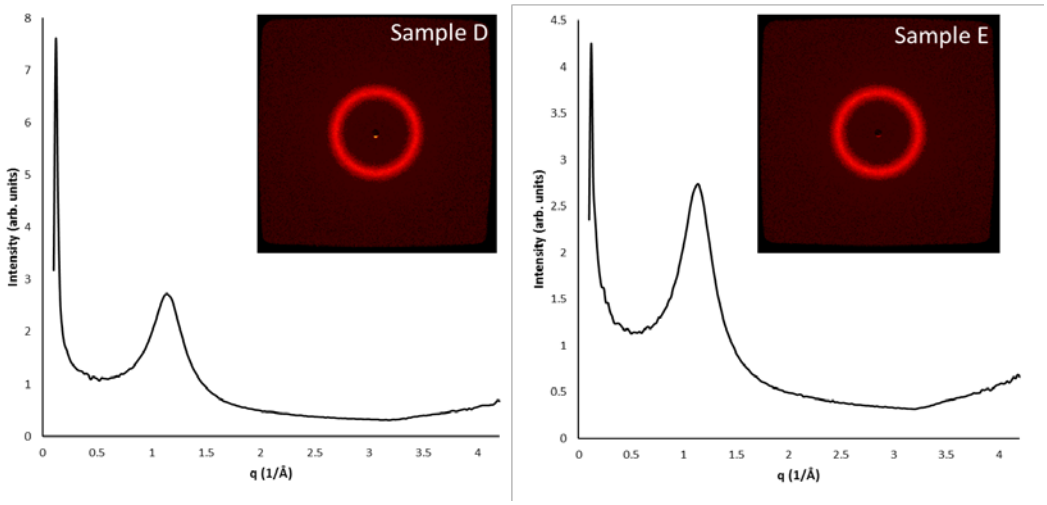


Figure 16. SAXS spectrum obtained from samples D and E with hexagonal pattern. Insets show 2D SAXS images

One important point for making membrane is that mesophases keep their structure during polymerization. Additionally, since thermal initiation is used beside photo initiation, we need to make sure mesophases preserve their structure during heating.

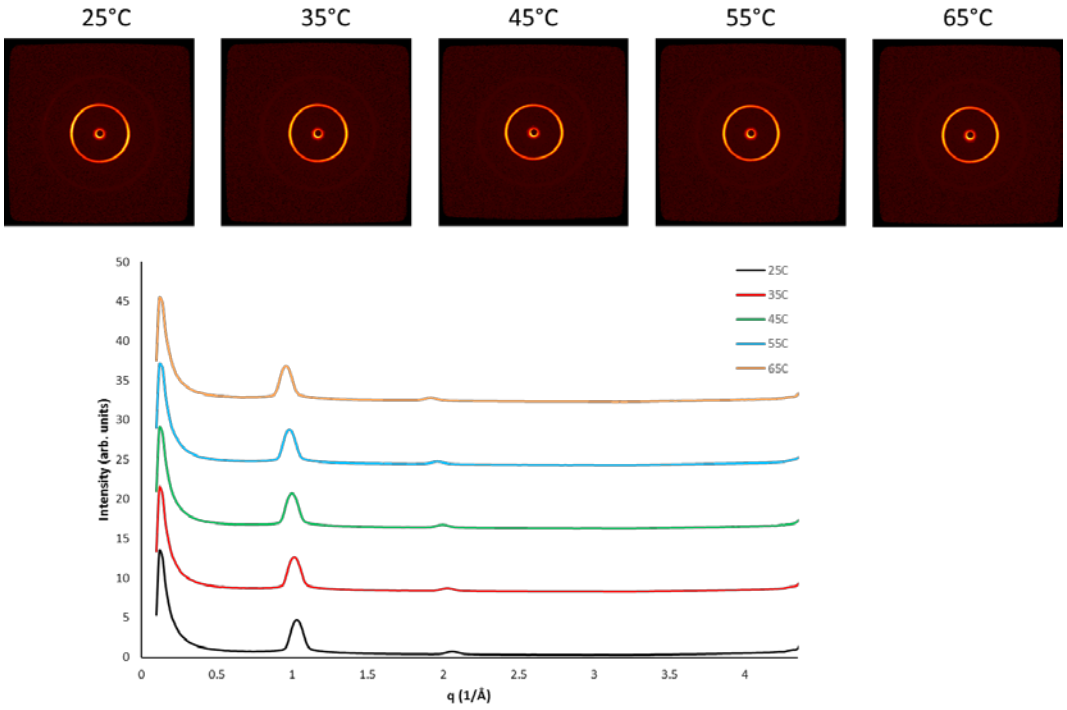


Figure 17. SAXS spectra of sample A at different temperatures

Figure 17 shows the SAXS spectra of sample A at different temperatures. It can be seen that the structure remains intact up to 65°C which proves that using thermal initiation is safe for polymerization of mesophases. Therefore, the scale-up of such membrane fabrication process will be possible.

The produced samples have mesostructure in the range of 70 nm as calculated from Bragg's law.

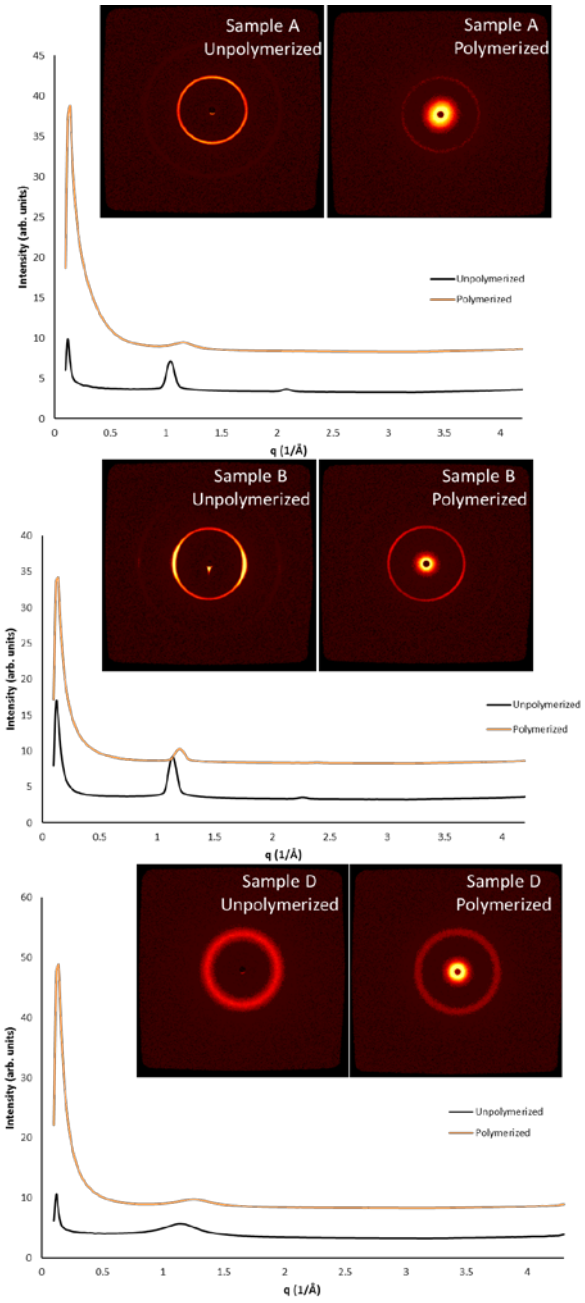


Figure 18. SAXS spectra of samples A, B, and D before and after polymerization

Figure 18 shows the SAXS spectra of samples A, B, and D after polymerization, respectively. As seen, the structure of mesophases remains intact during curing and the polymerized samples have a mesoporous structure at the end. Polymerization usually results in losing one order of crystallinity that is the case here. Additionally, the intensity of the peaks declines upon polymerization due to less ordering, and position of peaks may slightly shift as well.

### 3.3. Rheology results

All rheological measurements were performed on samples A and D that are located in lamellar and hexagonal regions, respectively. Figure 19 shows the variation of storage modulus, G', and loss modulus, G", versus strain. Storage modulus shows the significance of elastic behavior in materials, while loss modulus is a result of energy dissipation. The viscosity can be calculated form storage and loss moduli as follows:

$$G^* = G' + iG''$$

$$|\eta^*| = \frac{\sqrt{G'^2 + G''^2}}{\omega}$$

where G*, |η*|, and ω are dynamic complex modulus, magnitude of complex viscosity, and angular frequency, respectively.

The results in Figure 19 show Type III non-linear behavior for both systems. Weak strain overshoot and a local maximum in G'' are two important characteristics of such behavior. Polymer solution systems, block copolymer solutions, and highly concentrated emulsion also show such behavior.[46] It can be

seen that hexagonal structure in sample D shows about one order of magnitude higher moduli compared to lamellar structure in sample A.

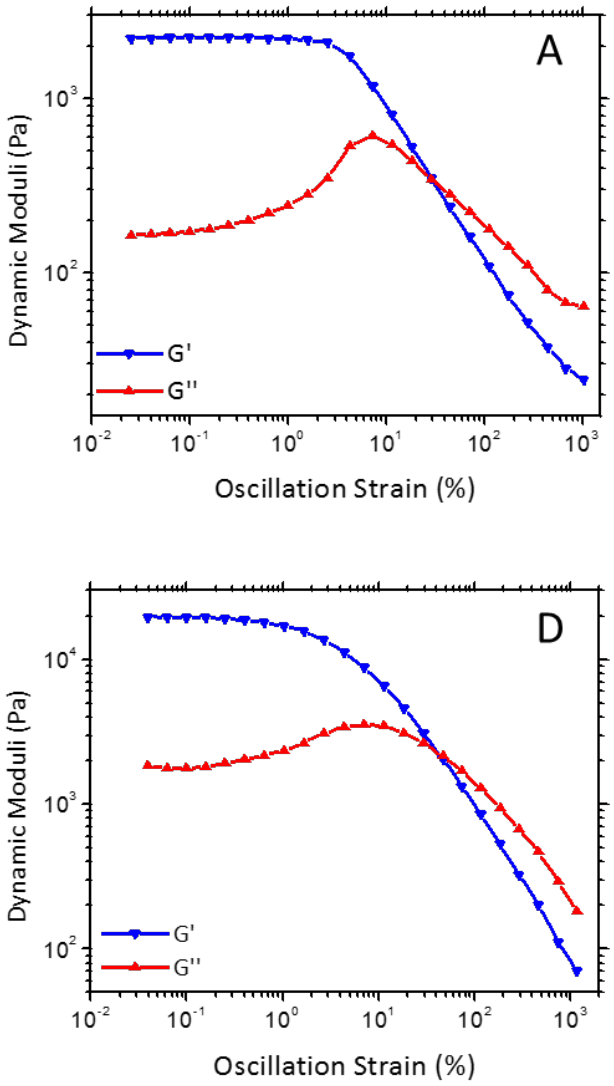


Figure 19. Storage modulus, G', and loss modulus, G", versus strain obtained through oscillatory amplitude sweep experiments on samples A and D

Figure 20 shows the frequency sweep data of sample A and D obtained from small amplitude oscillatory shear experiments. Both samples show solid-like behavior since G'>G". The storage and loss moduli of sample D are one order of magnitude higher than that of sample A. High complex viscosity in both samples shows that they cannot be processed by lab-scale doctor blade film applicator. Instead, we used hot press to make membranes in this work.

Although linear viscoelasticity is useful for understanding the relationship between the microstructure and the rheological properties of complex fluids, it is important to bear in mind that the linear viscoelasticity theory is only valid when the total deformation is quite small. However, in most processing operations the deformation is both large and rapid (therefore in the nonlinear region). Consequently, linear viscoelastic characterization is not sufficient to fully understand practical polymer processing undergoing nonlinear situations. Moreover, since linear viscoelastic experiments use small amplitude oscillatory shear (SAOS test), it has a limited resolution to distinguish complex fluids with similar micro- and nano-structure or molecular structures (e.g. linear or branched polymer topology). Complex fluids with similar linear viscoelastic properties may show different nonlinear viscoelastic properties. This means that even if rheological measurements are only being used for material characterization or quality control, the linear viscoelastic properties may often be insufficient. It can be anticipated that nonlinear viscoelastic characterization will provide much more insight for distinguishing such structural differences.

Thus, it is necessary to study the nonlinear viscoelastic responses of complex fluids in depth.

Figure 21 shows a schematic illustration of the strain sweep test at a fixed frequency. In the linear region, the storage (G') and loss (G'') moduli are independent of the applied strain amplitude at a fixed frequency and the resulting stress is a sinusoidal wave. However, in the nonlinear region, the storage and loss moduli become a function of the strain amplitude, $G'(\gamma_0)$ and $G''(\gamma_0)$, at a fixed frequency and the resulting stress waveforms are distorted from sinusoidal waves. While the SAOS is in the linear region , the application of large amplitude oscillatory shear (LAOS) results in a nonlinear material response.[47]

Large amplitude oscillatory shear (LAOS) data, which represents non-linear viscoelastic behavior, are shown in Figure 22. Figure 22a and c represent oscillatory stress versus time and Figure 22b and d show closed-loop of stress versus strain plots (also known as Lissajous plots). Oscillatory stress plot of sample A shows backward tilted stress, while sample D shows saw tooth stress. Closed-loop plots of two samples are completely different, especially at high shear stresses, which may be considered as fingerprints for lamellar and hexagonal mesostructures. In other words, in addition to SAXS and PLM, rheological measurements can be used to distinguish different mesophases.

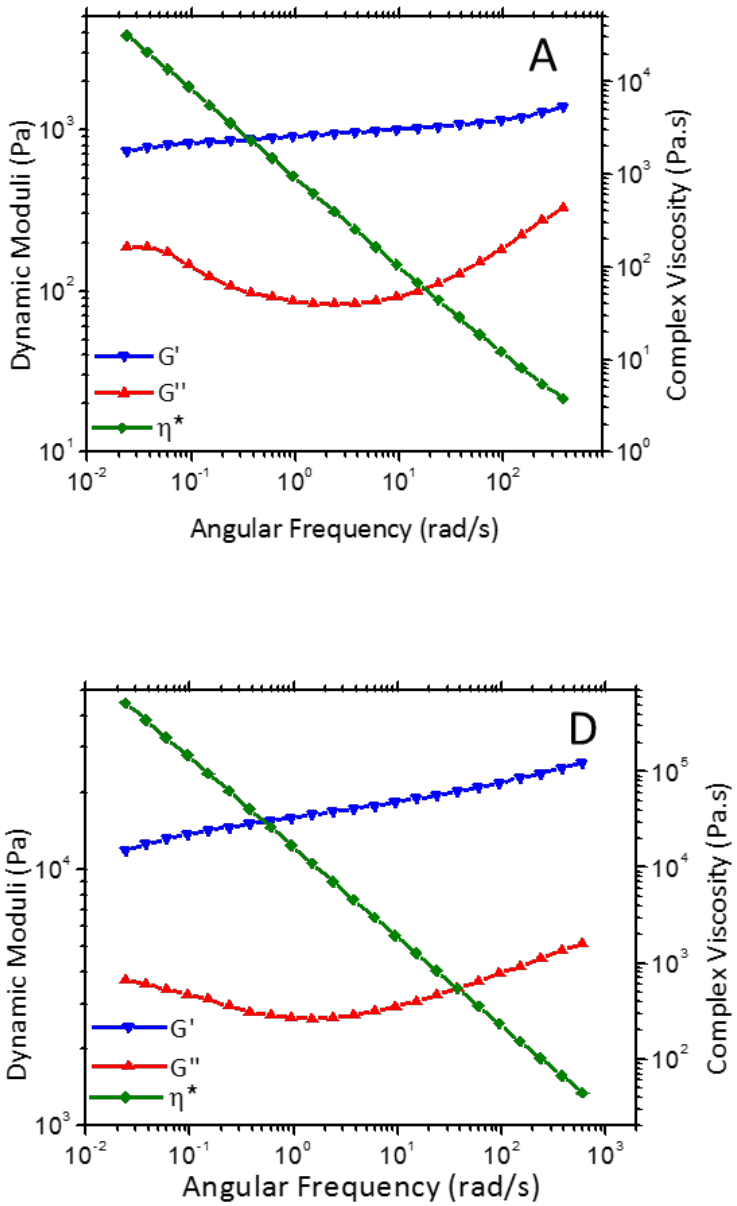


Figure 20. Storage modulus, G', loss modulus, G'', and complex viscosity, $\eta^*$, versus angular frequency of samples A and D obtained through frequency sweep in small oscillatory amplitude shear regime

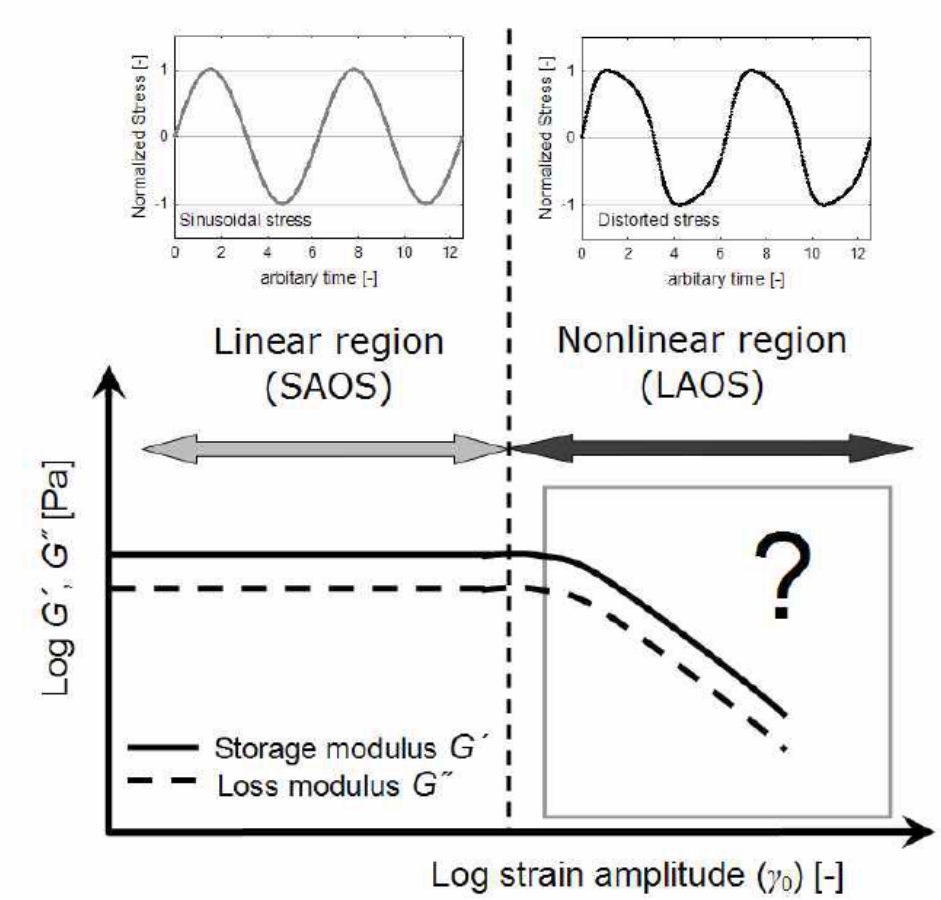


Figure 21. Schematic illustration of the strain sweep test at a fixed frequency[47]

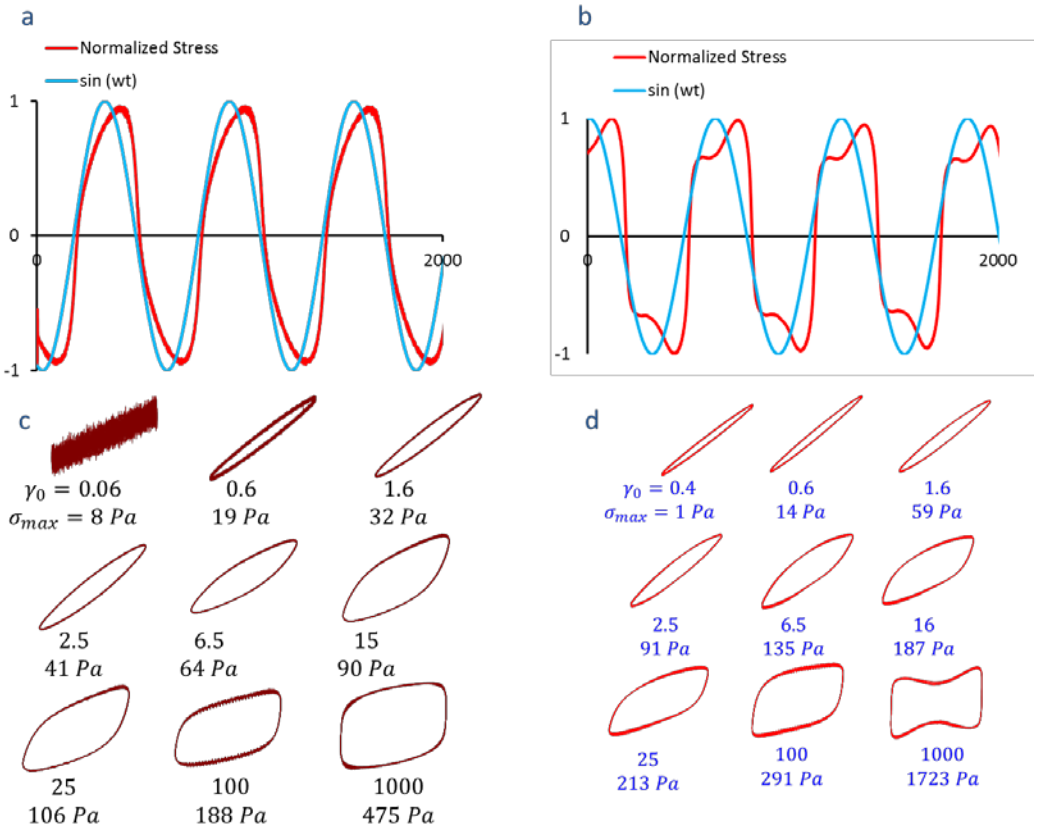


Figure 22. Oscillatory stress curves versus time (a ,b), and closed-loop plots of normalized stress versus normalized strain (c,d) obtained from amplitude oscillation in large amplitude oscillatory shear regime. a and c plots represent sample A and b and d plots represent sample D

### 3.4. Permeability results

Table 3 shows the obtained permeability results performed by the home-made filtration unit. Membranes A and D have two different mesostructures. As characterized by different techniques, membrane 1 composition (sample A) lies in lamellar region, while membrane 2 composition (sample D) lies in hexagonal region. As Table 3 shows, membrane 1 and 2 have higher permeability compared

to commercial membrane (GE, MW series, MW2540F30) that indicates better performance of fabricated membranes. It should be noted that the mesophase templated membranes were cast on the support layer recovered from GE MW2540F30 membrane in order to cancel the effect of support on the obtained results.

Table 3. Permeability results for membranes

| | Commercial membrane (GE, MW2540F30) | Support | Membrane A | Membrane D |
|---|---|---|---|---|
| Q (ml/s) | 1 | 33.33 | 47.619 | 35.088 |
| μ (mPa.s) | 1.002 | 1.002 | 1.002 | 1.002 |
| A ($mm^2$) | 1380 | 1380 | 1380 | 1380 |
| ΔP (kPa) | 1099 | 32.05 | 749 | 989 |
| l (mm) | 0.21 | 0.11 | 0.14 | 0.14 |
| κ/l ($ml/mm^2$) | $6.61\times10^{-13}$ | $7.55\times10^{-10}$ | $4.62\times10^{-11}$ | $2.58\times10^{-11}$ |

### 3.5. Rejection Results

2 g/L talc in water was used as feed solution. Talc concentration in the feed and permeate was measured and solute particle rejection (r) was calculated based on the following equation:

$$r = 1 - \frac{C_p}{C_f} \times 100\%$$

where, $C_p$ and $C_f$ are the concentrations of permeate and feed, respectively. Talc rejection of membranes A and D were measured to be about 99.9% that shows excellent rejection performance of the membranes for suspended particles. Figure 23 shows membrane A before and after rejection test. As seen, a cake layer of talc has formed on the surface of membrane. It should be noted that after 90 min of filtering 2g/L talc suspension, the permeate flow rate reaches zero due to the formation of cake in dead-end configuration of setup.

Rejection performance was also tested for an oil-in-water emulsion (with ~2.4 wt.% oil and prepared as described in the Experimental section) as feed. Oil concentration in permeate and feed streams were measured through centrifugation. The rejection of membrane for the emulsion sample was calculated to be about 65%. The lower rejection here compared to talc suspension can be attributed to the dead-end configuration of set-up, which results in significant increase in filtration pressure and forcing the liquid oil droplets to pass through pores of membrane. It is expected to have a much higher rejection in the cross-flow configuration, where oil droplet will not be pushed through pore of membrane.

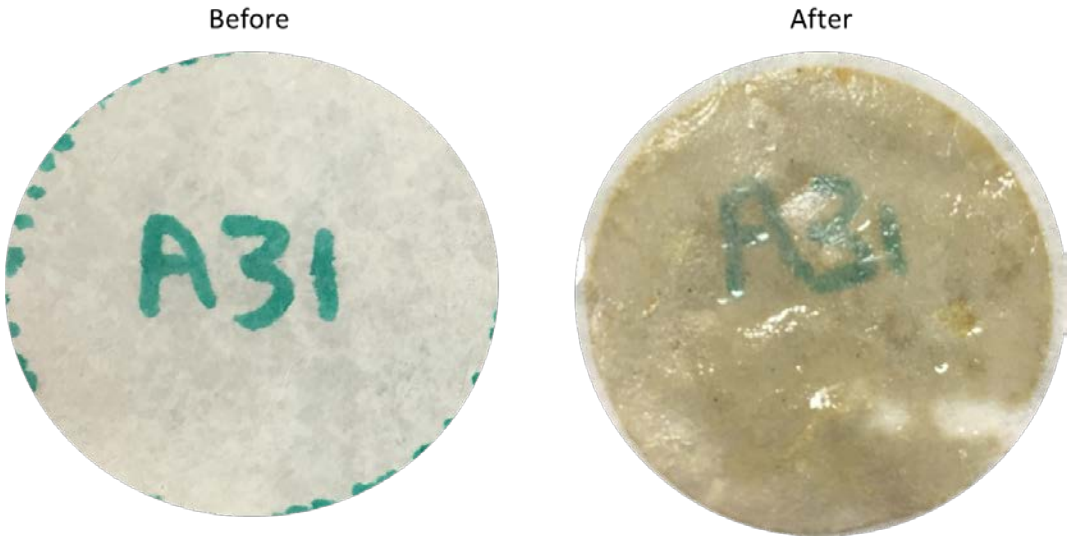


Figure 23.membrane surface appearance before and after rejection test with 2 wt.% talc suspension. A cake layer of talc was formed on the membrane surface after the test.

## 4. Conclusion

Surfactant self-assembly in the presence of water/oil was used as a template for making UF membranes. Different formulations were tried for oil phase and the optimum cross-linker (ethylene glycol dimethacrylate) and initiator were obtained at 70 wt.% of monomer (butyl acrylate) and 5 wt.% of monomer, respectively. UV (1-hydroxycyclohexyl phenyl ketone) and thermal (AIBN) initiators were used in conjunction for polymerizing mesophases. Cross-polarized light microscopy, SAXS, and rheology were used for characterizing samples. Membranes were cast on a support recovered from a commercially available UF membrane (GE, MW series, MW2540F30). The produced membranes have mesopores in the range of 70 nm according to SAXS measurements. The

permeability and rejection performance of membranes were evaluated by using a home-made dead-end setup. The results indicate that fabricated membranes have higher permeability compared to commercial UF membranes. In addition, 2 g/L talc suspension and 2.4 wt.% oil-in-water emulsion were used to test the rejection performance of the membranes in the dead-end setup. Rejection was calculated to be about 99.9% and 65% for talc suspension and oil-in-water emulsion, respectively. These results confirm that mesophase templated polymers have the potential to be used as ultrafiltration membranes and can be further developed for such applications.

## 5. Future wok

Proposed templating approach is viable for any type of monomer. More hydrophilic monomers could be used in future to improve the permeability of the membranes. Besides, using both hydrophobic and hydrophilic monomers is proposed. Hydrophilic monomers would be added to aqueous phase and guarantee the high permeability, while hydrophobic monomers strengthen the membrane and make it insoluble in water. Rejection performance of the membranes may be done using other feed streams for example proteins and viruses.

## References

(1) http://www.un.org/waterforlifedecade/scarcity.shtml
http://www.un.org/waterforlifedecade/scarcity.shtml.

(2) Baker, R. W. *Membrane Technology and Applications*; 2nd editio.; John Wiley & Sons, Ltd.: Chichester, UK, 2004.

(3) Loeb, G. S.; Sourirajan, S. Sea Water Demineralization by Means of an Osmotic Membrane. *Adv. Chem. Ser* **1968**, *38*, 117.

(4) Guillen, G. R.; Pan, Y.; Li, M.; Hoek, E. M. V. Preparation and Characterization of Membranes Formed by Nonsolvent Induced Phase Separation: A Review. *Ind. Eng. Chem. Res.* **2011**, *50*, 3798–3817.

(5) Tsai, H. Effect of Surfactant Addition on the Morphology and Pervaporation Performance of Asymmetric Polysulfone Membranes. *J. Memb. Sci.* **2000**, *176*, 97–103.

(6) Chakrabarty, B.; Ghoshal, A. K.; Purkait, M. K. Preparation, Characterization and Performance Studies of Polysulfone Membranes Using PVP as an Additive. *J. Memb. Sci.* **2008**, *315*, 36–47.

(7) Barth, C.; Gonçalves, M. C.; Pires, A. T. N.; Roeder, J.; Wolf, B. A. Asymmetric Polysulfone and Polyethersulfone Membranes: Effects of Thermodynamic Conditions during Formation on Their Performance. *J. Memb. Sci.* **2000**, *169*, 287–299.

(8) IUPAC Manual of Symbols and Terminology. *Pure Appl. Chem* **1972**, *31*, 578.

(9) Feng, P.; Bu, X.; Pine, D. J. Control of Pore Sizes in Mesoporous Silica Templated by Liquid Crystals in Block Copolymer−Cosurfactant−Water Systems. *Langmuir* **2000**, *16*, 5304–5310.

(10) Li, W.; Zhao, D. An Overview of the Synthesis of Ordered Mesoporous Materials. *Chem. Commun. (Camb).* **2013**, *49*, 943–946.

(11) Tolbert, S. H. Magnetic Field Alignment of Ordered Silicate-Surfactant Composites and Mesoporous Silica. *Science (80-. ).* **1997**, *278*, 264–268.

(12) Gin, D. L.; Gu, W. Nanoporous Catalytic Materials with Organic Frameworks. *Adv. Mater.* **2001**, *13*, 1407–1410.

(13) Lester, C. L.; Colson, C. D.; Guymon, C. A. Photopolymerization Kinetics and Structure Development of Templated Lyotropic Liquid Crystalline Systems. *Macromolecules* **2001**, *34*, 4430–4438.

(14) Gin, D. L.; Gu, W.; Pindzola, B. A.; Zhou, W.-J. Polymerized Lyotropic Liquid Crystal Assemblies for Materials Applications. *Acc. Chem. Res.* **2001**, *34*, 973–980.

(15) Mann, S.; Burkett, S. L.; Davis, S. A.; Fowler, C. E.; Mendelson, N. H.; Sims, S. D.; Walsh, D.; Whilton, N. T. Sol−Gel Synthesis of Organized Matter. *Chem. Mater.* **1997**, *9*, 2300–2310.

(16) Hentze, H.-P.; Kaler, E. W. Polymerization of and within Self-Organized Media. *Curr. Opin. Colloid Interface Sci.* **2003**, *8*, 164–178.

(17) Hentze, H.-P.; Kaler, E. W. Morphosynthesis of Nanostructured Polymer Gels by Polymerization within Reverse Hexagonal Mesophases. *Chem. Mater.* **2003**, *15*, 708–713.

(18) Tiddy, G. Surfactant-Water Liquid Crystal Phases. *Phys. Rep.* **1980**, *57*, 1–46.

(19) Antonietti, M.; Caruso, R. A.; Göltner, C. G.; Weissenberger, M. C. Morphology Variation of Porous Polymer Gels by Polymerization in Lyotropic Surfactant Phases. *Macromolecules* **1999**, *32*, 1383–1389.

(20) McGrath, K. M.; Drummond, C. J. Polymerisation of Liquid Crystalline Phases in Binary Surfactant/water Systems. *Colloid Polym. Sci.* **1996**, *274*, 316–333.

(21) McGrath, K. M. Polymerisation of Liquid Crystalline Phases in Binary Surfactant/water Systems. *Colloid Polym. Sci.* **1996**, *274*, 499–512.

(22) McGrath, K. M.; Drummond, C. J. Polymerisation of Liquid Crystalline Phases in Binary Surfactant/water Systems. *Colloid Polym. Sci.* **1996**, *274*, 612–621.

(23) Srisiri, W.; Sisson, T. M.; O'Brien, D. F.; McGrath, K. M.; Han, Y.; Gruner, S. M. Polymerization of the Inverted Hexagonal Phase. *J. Am. Chem. Soc.* **1997**, *119*, 4866–4873.

(24) Guymon, C. A.; Bowman, C. N. Kinetic Analysis of Polymerization Rate Acceleration During the Formation of Polymer/Smectic Liquid Crystal Composites. *Macromolecules* **1997**, *30*, 5271–5278.

(25) H. T. Davis, J. F. Bodet, L. E. Scriven, W. G. M. *Microemulsions and Their Precursors*; Meunier, J.; Langevin, D.; Boccara, N., Eds.; Springer Proceedings in Physics; Springer Berlin Heidelberg: Berlin, Heidelberg, 1987; Vol. 21.

(26) Liu, J.; Kim, A. Y.; Wang, L. Q.; Palmer, B. J.; Chen, Y. L.; Bruinsma, P.; Bunker, B. C.; Exarhos, G. J.; Graff, G. L.; Rieke, P. C.; *et al.* Self-Assembly in the Synthesis of Ceramic Materials and Composites. *Adv. Colloid Interface Sci.* **1996**, *69*, 131–180.

(27) Letchford, K.; Burt, H. A Review of the Formation and Classification of Amphiphilic Block Copolymer Nanoparticulate Structures: Micelles, Nanospheres, Nanocapsules and Polymersomes. *Eur. J. Pharm. Biopharm.* **2007**, *65*, 259–269.

(28) Liu, S.; Armes, S. P. Recent Advances in the Synthesis of Polymeric Surfactants. *Curr. Opin. Colloid Interface Sci.* **2001**, *6*, 249–256.

(29) Fenyves, R.; Schmutz, M.; Horner, I. J.; Bright, F. V; Rzayev, J. Aqueous Self-Assembly of Giant Bottlebrush Block Copolymer Surfactants as Shape-Tunable Building Blocks. *J. Am. Chem. Soc.* **2014**, *136*, 7762–7770.

(30) Khandpur, A. K.; Foerster, S.; Bates, F. S.; Hamley, I. W.; Ryan, A. J.; Bras, W.; Almdal, K.; Mortensen, K. Polyisoprene-Polystyrene Diblock Copolymer Phase Diagram near the Order-Disorder Transition. *Macromolecules* **1995**, *28*, 8796–8806.

(31) Lohse, D. J.; Hadjichristidis, N. Microphase Separation in Block Copolymers. *Curr. Opin. Colloid Interface Sci.* **1997**, *2*, 171–176.

(32) Alexandridis, P.; Alan Hatton, T. Poly(ethylene Oxide) □poly(propylene Oxide) □poly(ethylene Oxide) Blo and at Interfaces: Thermodynamics, Structure, Dynamics, and Modeling. *Colloids Surfaces A Physicochem. Eng. Asp.* **1995**, *96*, 1–46.

(33) Hentze, H.-P.; Krämer, E.; Berton, B.; Förster, S.; Antonietti, M.; Dreja, M. Lyotropic Mesophases of Poly(ethylene Oxide)- B -Poly(butadiene) Diblock

Copolymers and Their Cross-Linking To Generate Ordered Gels. *Macromolecules* **1999**, *32*, 5803–5809.

(34) Alexandridis, P.; Lindman, B. *Amphiphilic Block Copolymers: Self-Assembly and Application*; Elsevier, 2000.

(35) Bates, F. S. Polymer-Polymer Phase Behavior. *Science* **1991**, *251*, 898–905.

(36) Alexandridis, P. Amphiphilic Copolymers and Their Applications. *Curr. Opin. Colloid Interface Sci.* **1996**, *1*, 490–501.

(37) Mortensen, K.; Brown, W.; Nordén, B. Inverse Melting Transition and Evidence of Three-Dimensional Cubatic Structure in a Block-Copolymer Micellar System. *Phys. Rev. Lett.* **1992**, *68*, 2340–2343.

(38) Svensson, B.; Olsson, U.; Alexandridis, P. Self-Assembly of Block Copolymers in Selective Solvents: Influence of Relative Block Size on Phase Behavior. *Langmuir* **2000**, *16*, 6839–6846.

(39) Alexandridis, P.; Olsson, U.; Lindman, B. Phase Behavior of Amphiphilic Block Copolymers in Water−Oil Mixtures: The Pluronic 25R4−Water− P -Xylene System. *J. Phys. Chem.* **1996**, *100*, 280–288.

(40) Alexandridis, P.; Olsson, U.; Lindman, B. Self-Assembly of Amphiphilic Block Copolymers: The (EO)13(PO)30(EO)13-Water-P-Xylene System. *Macromolecules* **1995**, *28*, 7700–7710.

(41) Holmqvist, P.; Alexandridis, P.; Lindman, B. Phase Behavior and Structure of Ternary Amphiphilic Block Copolymer−Alkanol−Water Systems: Comparison of Poly(ethylene oxide)/Poly(propylene Oxide) to Poly(ethylene oxide)/Poly(tetrahydrofuran) Copolymers. *Langmuir* **1997**, *13*, 2471–2479.

(42) Alexandridis, P.; Olsson, U.; Lindman, B. Structural Polymorphism of Amphiphilic Copolymers: Six Lyotropic Liquid Crystalline and Two Solution Phases in a Poly(oxybutylene)- B -poly(oxyethylene)−Water−Xylene System. *Langmuir* **1997**, *13*, 23–34.

(43) Bilalov, A.; Olsson, U.; Lindman, B. Complexation between DNA and Surfactants and Lipids: Phase Behavior and Molecular Organization. *Soft Matter* **2012**, *8*, 11022.

(44) http://micro.magnet.fsu.edu/primer/techniques/polarized/configuration.html http://micro.magnet.fsu.edu/primer/techniques/polarized/configuration.html.

(45) S., H. *Identification of Lyotropic Liquid Crystal Mesophases, Chap 1. In: Holmberg (ed) Handbook of Applied Surface and Colloid Chemistry*; Wiley, New York, 2001.

(46) Foudazi, R.; Masalova, I.; Malkin, A. Y. The Rheology of Binary Mixtures of Highly Concentrated Emulsions: Effect of Droplet Size Ratio. *J. Rheol. (N. Y. N. Y).* **2012**, *56*, 1299.

(47) Hyun, K.; Wilhelm, M.; Klein, C. O.; Cho, K. S.; Nam, J. G.; Ahn, K. H.; Lee, S. J.; Ewoldt, R. H.; McKinley, G. H. A Review of Nonlinear Oscillatory Shear Tests: Analysis and Application of Large Amplitude Oscillatory Shear (LAOS). *Prog. Polym. Sci.* **2011**, *36*, 1697–1753.